



Distributed Fibre Optic Sensing (DFOS) in 3D small-scale tests on steel-reinforced piled embankments

Suzanne J.M. van Eekelen¹, Marc Schneider², Marylin Hell³, Karolina Makowska⁴, Katarzyna Zdanowicz⁵,
Britt Wittekoek¹, Paul Pandrea³, Rafał Sieńko⁴, Pascal Schaubert³, Michał Topolnicki⁶, Hauke Zachert²

¹*Deltares, Delft, Netherlands, suzanne.vaneekelen@deltares.nl, britt.wittekoek@deltares.nl,*

²*Technical University of Darmstadt, Faculty of Civil and Environmental Engineering, Institute of Geotechnics,
Germany, marc.schneider1@tu-darmstadt.de, hauke.zachert@tu-darmstadt.de,*

³*Keller Holding GmbH, Germany, marylin.hell@keller.com, paul.pandrea@keller.com,*

⁴*SHM System, Poland, km@shmsystem.pl, rs@shmsystem.pl,*

⁵*FOLAB GmbH, Germany, k.zdanowicz@folab.de, ⁶Keller Polska, Poland, michal.topolnicki@keller.com*

ABSTRACT: This paper explores the application of Distributed Fibre Optic Sensing (DFOS) technology in a series of small-scale tests on steel-reinforced piled embankments. The tests were conducted as part of a study on the impact of welded steel mesh reinforcement on soil arching, settlement patterns, and strain distribution. DFOS technology played a key role, providing a detailed 3D perspective on the strains and deformations of the reinforcement and soil at various levels in the fill. While DFOS measurements have high precision, occasional local spikes (deviations or strain reading anomalies (SRAs)) were observed, necessitating careful interpretation. The interpretation procedures employed may affect the results. The paper discusses these procedures, addressing challenges such as handling spikes and determining 3D deformations from strain measurements. Recommendations for future DFOS applications in similar contexts are provided. Besides the extensive benefits provided by the innovative DFOS technology for geotechnical experimental research, this paper thoroughly discusses the challenges and limitations in data interpretation. Insights gained from small-scale tests at Deltares were used to detail the large-scale test set-up of a piled embankment at Technical University of Darmstadt, Germany.

1 DFOS MEASUREMENTS IN STEEL MESH BASAL REINFORCED PILED EMBANKMENTS

Pile-supported (PS) embankments with basal geosynthetic reinforcement (GR) are commonly built in soft soil areas (van Eekelen and Han, 2020). Steel mesh reinforcement (SR) offers advantages for high embankments, as highlighted in Topolnicki et al. (2019). The high axial stiffness of SR, compared to geosynthetic, reduces horizontal deformation at the embankment base, minimizes bending moments in the piles, ultimately enhancing embankment stability.

Van Eekelen et al., 2024, presented a small-scale test series on steel-reinforced piled embankments. The tests are part of a research initiative called Piled Embankments with Basal Steel Reinforcement (PEBSTER), which also includes a large-scale test (Schneider et al., 2024a and b).

DFOS technology played a key role in these tests by providing a detailed 3D perspective on the strains and deformations of both the reinforcement and the fill. The DFOS measurements included steel strains,

soil strains and 3D deformation at different levels within the fill. The 3D deformation was calculated from strains measured by four optical fibres that were attached together in a 3DSensor on a flexible plastic frame. Despite their high accuracy, the measurements showed occasional local spikes, also known as strain reading anomalies (SRAs). Additionally, the interpretation of 3D deformations required careful consideration. While *differential* deformations were determined relatively easily, specific procedures had to be applied to determine the *absolute* 3D deformations along the DFOS sensors.

The paper thoroughly discusses the decision-making process and procedures followed during the analysis and interpretation of the DFOS data.

This paper aims to address the following questions:

- How to handle local spikes in measurements?
- How to determine absolute 3D deformations from 3D differential deformations and measured deformations at the reference points?
- What recommendations can be made for future DFOS applications in similar contexts?

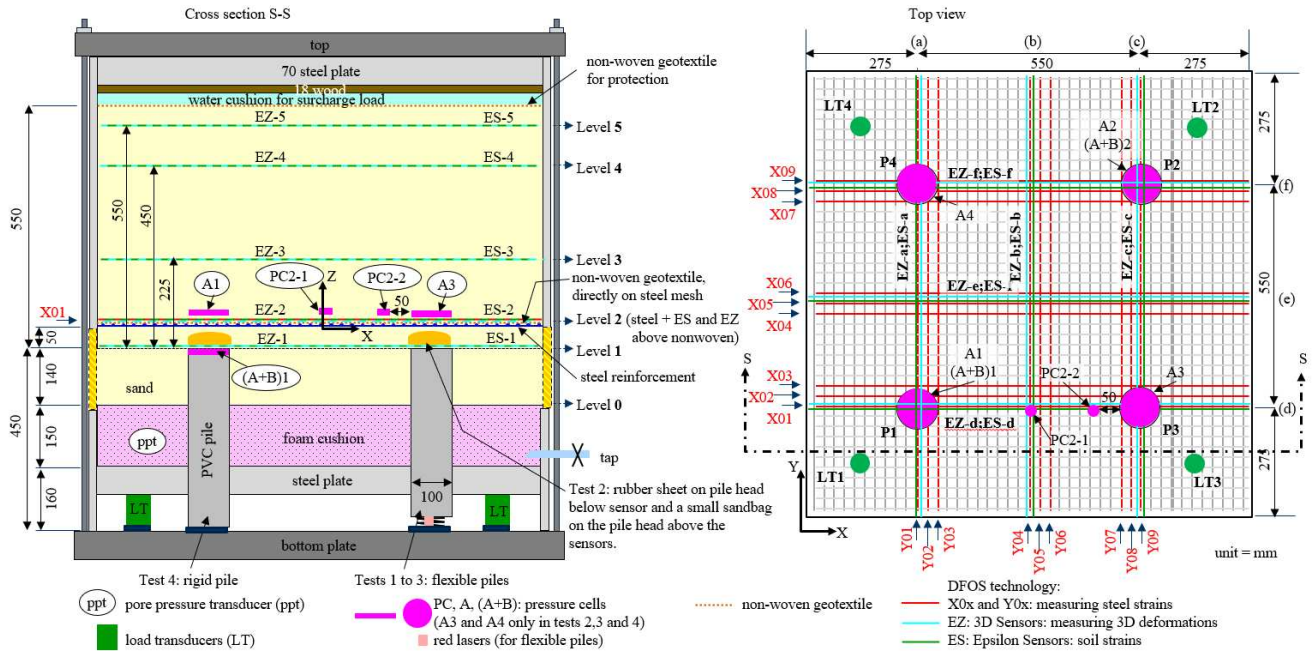


Figure 1. Test set-up of the small-scale test on steel-reinforced pile-supported embankments. Source: van Eekelen et al., 2024.

2 SET-UP SMALL-SCALE TESTS

Figure 1 shows the test set-up, previously described by van Eekelen et al. (2024). It is an extended version of the test set-up described by Van Eekelen et al. (2012 and 2024) and Van Eekelen (2024). A steel plate supports a sealed and saturated foam cushion. Drainage of the foam cushion through a tap simulated the consolidation of the subsoil between the piles. Four piles with a 0.1 m diameter pass through the steel plate.

The welded steel mesh-reinforcement was placed 50 mm above the pile heads. It consists of 43 bars in each direction. These bars have a 5 mm diameter and a centre-to-centre spacing of 25 mm, resulting in an axial stiffness $EA = 164934 \text{ kN/m}$ and bending stiffness $EI = 0.2577 \text{ kN}\cdot\text{m}^2$.

The fill material, ‘Darmstadt sand’, consists of sediments from the river Main and is characterized as medium coarse sand. Table 1 lists test details, where the values of φ'_{cv} were derived from the relative density of the fill, using an empirical correlation obtained from 15 triaxial tests conducted at Technical University Darmstadt.

Table 1. Test details of the four small-scale tests.

Test no.	1	2	3	4
Fill height above steel (m)	0.55	0.55	0.55	0.56
Unit weight γ (kN/m ³)	16.7	16.9	17.0	16.6
Relative density RD (%)	68	72	75	64
Friction angle φ'_{cv} (°)	33.8	34.0	34.1	33.7

An equally distributed surcharge load was applied using a water cushion. A rubber sheet greased with

Vaseline and a rubber sleeve minimised the friction between fill, box walls, foam cushion and piles. The load distribution was measured by pressure cells and load transducers. Van Eekelen et al., 2024 presented their results. This paper delves into the strains and deformations that were measured using DFOS technology, and discussed the work undertaken to ensure reliable interpretation of the measurements.

The test series included four tests. The first included SR, flexible piles (utilizing springs with a stiffness of 4605 kN/m below the piles) and stepwise consolidation and is presented here.

3 THREE TYPES OF DFOS MEASUREMENTS

Strains and displacements were monitored utilizing Distributed Fibre Optic Sensing (DFOS) technology, for which sensors from the Nerve-Sensors family were used. These sensors provided a unique insight in the strains and deformations within the soil body. The following three types of DFOS sensors were used:

- 3DSensors measured the settlements at five elevations within the fill (Figure 1). The sensors each consisted of four parallel optic fibres cast into a flexible plastic frame (Figure 2). The fibres measure strains, from which the differential deformations along the sensor were calculated. To determine the absolute settlements from these differential settlements, simultaneous measurement of the vertical movement of reference points was necessary. Section 5 further looks at these deformation measurements.

- EpsilonSensors measured soil strains (Figure 2). They were loosely attached to the plastic frame of the 3DSensors, using small tie wraps.
- Acrylate-coated optical fibres were glued to the steel mesh reinforcement to measure the strains in the steel (Figure 3). In the x-direction, X01 to X09 were glued to the top of the top steel bars.

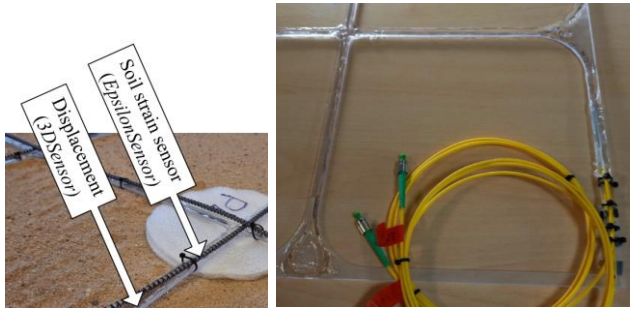


Figure 2. Left: EpsilonSensors (measuring soil strains) and 3DSensors (measuring 3D deformations), they were cast into a flexible plastic frame. Right: Detail 3DSensors.



Figure 3. Fibre optic sensors measuring steel reinforcement strain (yellow tubes were used for protection of the acrylate-coated fibres in sections where fibres needed to be bent).

4 SPIKES IN THE DFOS MEASUREMENTS

4.1 Spikes: anomalous values in the data

Several of the optic fibre measurements show spikes. These are local deviations, anomalies or strain reading anomalies (SRAs) in the data. Usually, they are peaks up or down. Due to local optical phenomena in the fibres and limitations of the Rayleigh backscattering, the values deviated locally.

Figure 4 shows spikes in the measured steel strains as an example. The figure displays measurements taken during various test phases for two top-bars: X09, spanning the centre line of two piles, and X07, which extends just past two piles.

Bars spanning piles (like X09) experience stronger bending in the experiments and typically show more spikes than the bars along the piles (like X07).

The figure shows that more spikes occur when the load and the differential deformations increase and

where local pressure is exerted on the fibres, for example at the edges of the piles, as shown in Figure 4. Also, sensors positioned at higher levels in the fill show significantly less spikes, because smaller differential deformations occur at these heights. The spikes occur in all types of DFOS measurements in these experiments.

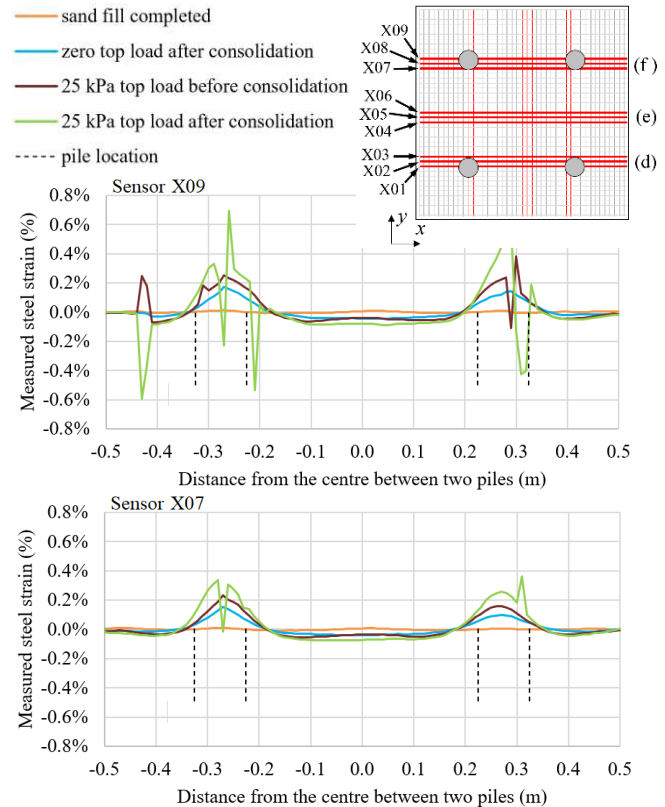


Figure 4 Measured steel strains at different phases of Test 1. Strains measured on top of the top steel bars in x-direction; top graph: across two piles (X09), bottom graph: along two piles (X07).

4.2 Why do spikes occur?

During the measurements, the Luna OBR 4600 reflectometer was utilized, which uses the Rayleigh scattering principle. The Rayleigh scattering occurs in optical fibres when light interacts with the structural inhomogeneities of the glass fibre. As a result of this interaction, a small fraction of the light is scattered in all directions. By sending a pulse of light down the fibre and analysing the backscattered light (the light scattered back towards the source), it is possible to determine the strain or temperature changes along the fibre. This technique is known as optical frequency domain reflectometry (OFDR). The changes in the backscatter pattern provide a detailed map of where and how the fibre is being affected.

When performing measurements using DFOS technology, spikes may appear that are not related to the actual behaviour of the tested element. These

spikes occur when the reading taken at a certain point significantly differs from the previous reading (in time).

A relatively high number of spikes were observed in specific locations where the optical fibres were locally heavily impacted:

- At levels 1 and 2, where sensors crossed the edge of the piles, the optical fibres were bent significantly, causing local disturbances in strain readings.
- In case of bare optical fibres glued to the steel mesh and displacement sensors in plastic frames, disturbances could have been further caused by local pressures of sand grains on the fibres as the protection of the optical fibre consisted only of a layer of adhesive to maintain the sensor stiffness as low as possible.

4.3 How to deal with the spikes?

The following methods were considered to deal with the spikes:

- I. Accept the spikes.
 - II. Remove the spikes, resulting in small gaps in the measurement curves.
 - III. Remove the spikes and interpolate the adjacent values, to create smooth curves.
 - IV. Use moving averages of the measured values.
- Each methodology has its advantages and disadvantages:

Method (I) has the disadvantage that experiment tendencies may be difficult to analyse, as illustrated in Figure 4. We can choose to focus on measurements with a limited number of spikes, especially those taken during the early test phases with limited surcharge loading or at higher elevations.

Method (II) requires identifying each incorrect value and manually removing it from the data. This is extremely time-consuming and leaves empty spaces in the data. Bado et al. (2020) give recommendations for algorithms to perform this removal automatically. These types of algorithms could be used with caution but was not done in this case.

Method (III) also requires manually finding the incorrect values, or a good algorithm as mentioned above, replacing them with interpolated values calculated from neighbouring strain values. In the conducted tests, a spatial resolution of 10 mm was adopted. Such a small distance between subsequent virtual sensors and knowledge of the sensors' locations relative to individual elements of the test setup allows for the safe assumption that the sought strain value could not have changed significantly from neighbouring values. In the case of individual spikes, the "error" made is small. However, in cases where

several incorrect consecutive values occur, it is possible to approximate the obtained values using a polynomial based on correct data from segments adjacent to the sought values. It should be considered that the longer the segment being interpolated, the less accurate the data we will receive based on the polynomial used. Consequently, this method requires a more detailed assessment of whether the assumed interpolated values are realistic, additionally based on measurements performed before and after the measurement under analysis.

Method (IV) is useful in situations where many spikes occur in subsequent gauges.

Bado et al. (2020) described more sophisticated fitting methods that can be used to maintain the reliability of the data.

During test data analyses, several methods were tried, and the following methods were finally chosen:

The steel strains were analysed using method (I), (Figure 4). Steel strains were analysed only up to a surcharge load of 25 kPa.

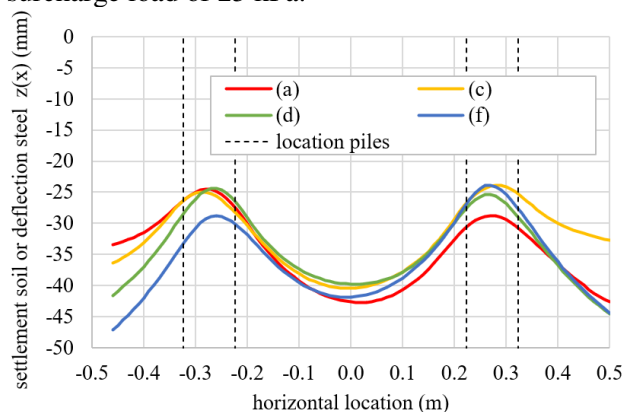


Figure 5. Test 1. 3DSensor results: measured settlements in the fill at level 2 (just above the steel mesh reinforcement), along lines (a), (b), (c) and (d), 75 kPa surcharge load, before the subsequent consolidation phase.

In calculating displacements from strains, recorded by 3DSensors (Figure 5), method (III) was necessary, because the displacement calculation algorithm is iterative and requires continuity of input data (Bednarski et al., 2021). However, it should be considered that the displacement calculation uses an averaged value not only from the same fibre, but also from the neighbouring fibre (so, it uses either two lower or two upper fibres).

If a spike appears in one out of the four fibres of the 3DSensor, and the distorted value is removed from the data, the algorithm will use the correct strain value from the remaining fibre on the top or the bottom of the grid with no spikes for the calculations. Using method (III) made it possible to present the results up to 75 kPa, and credibility of the measurements should again only be questioned in places where spikes occur.

Figure 6 compares the raw and processed soil strains and highlights the challenges due to the vast number of data, unusual spikes, the demand of precision and time constraints. As a result, the data was only partially cleaned and only elements that were undoubtedly spikes were removed. The figure shows that the red spike was removed, but the yellow spikes could not be interpreted and could therefore not be removed.

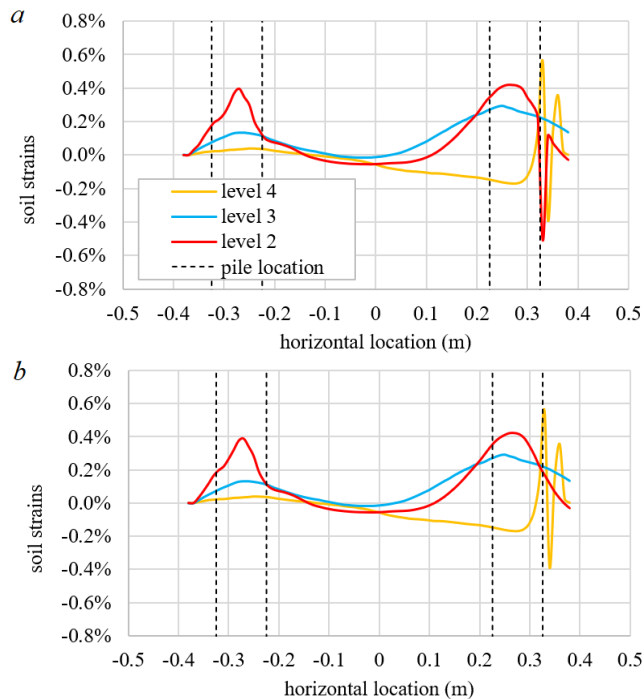


Figure 6. Sensor (a) of Test 1. Measured soil strains in the fill at various levels, surcharge load 75 kPa, before the subsequent consolidation phase. (a) raw data (b) processed data, where spikes were removed using method (III).

4.4 Conclusions data spikes

During the research planning phase, it was intended to use the same DFOS sensors in subsequent tests. However, due to significant forces in the system, and the way the optical fibre sensors were arranged, some sensors were damaged. Where possible, new optical fibre sensors were used for the subsequent test. For this reason, Test 1 provided the most measured data.

For future tests, it is recommended to prepare optical fibre sensors that are better protected against direct bending at sharp edges while ensuring that the sensors do not constitute additional reinforcement of the system, to foresee redundant separate optical fibre sensors in measurement lines located in areas of expected high strain values, and to provide additional protection for sensors in critical areas, using for example foam or springs.

5 DETERMINATION 3D DEFORMATIONS

3DSensors can be used to determine 3D deformations. Due to the primarily vertical deformation behaviour of the system, only vertical deformations (in z-direction) were considered.

5.1 Differential settlements

In the considered tests, each 3DSensor consisted of four optic fibres, that were cast into a flexible plastic frame as shown in Figure 2 and Figure 7. Figure 7 shows the two fibres that were glued on the upper side of the plastic frame. These two fibres were duplicated at the lower side, resulting in a total of four fibres. The four fibres each measure strain, and from this, the differential settlements along the sensor can be calculated (Bednarski et al. 2021).

5.2 Absolute settlements

The absolute settlements of a 3DSensor were determined from:

- The differential settlements measured by the four fibres in a 3DSensor as described above.
- The exact deformations measured at four reference points (RPs), indicated in Figure 7 and Figure 8.

The absolute position of the lines (a)-(f), at each moment and elevation was determined as follows:

- The absolute settlements along lines (b) and (e) were determined directly from the measured settlements at the four RPs at lines (b) and (e) and the differential settlements calculated from strain values along these lines.
- Lines (a) and (e) had equal deflections at their crossing (ae) because their fibres were cast into the same plastic frame. The same is true for all crossings bf, bd, ae and ce, enabling the derivation of the absolute settlement at the midpoints of lines (a), (c), (d) and (f).

The tilting of lines (a), (c), (d) and (f) was determined using a Monte Carlo analysis, minimizing differences in vertical displacement at the crossings above the four piles ((ad), (af), (cd), and (cf)). These differences deviate from zero due to the following factors:

- The accuracy assessment of fibre optic measurements depends on the sensor and the device used. Only straight sections were considered; turns marked as A and C in Figure 7 were not included in the calculations and were marked as non-measurable.
- RPs were installed at the edges of the sensors near box walls, while the measuring straight section ended a few cm from the edge. It was necessary to extrapolate displacements of the measuring area up to the reference points, which obviously could

impact the accuracy of the measured values. This observation led to an improved test setup in the subsequent large-scale tests (Schneider et al., 2024a and b).

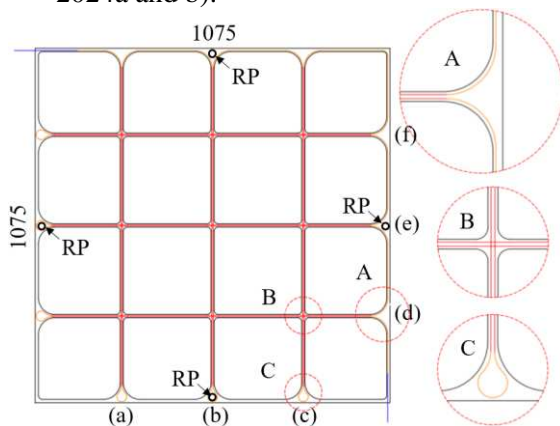


Figure 7. Plastic frame with 3DSensors. Upper and lower side are similar. RF = Reference Point. Sizes in mm. See also Figure 2 for a photo of edge types A and C.

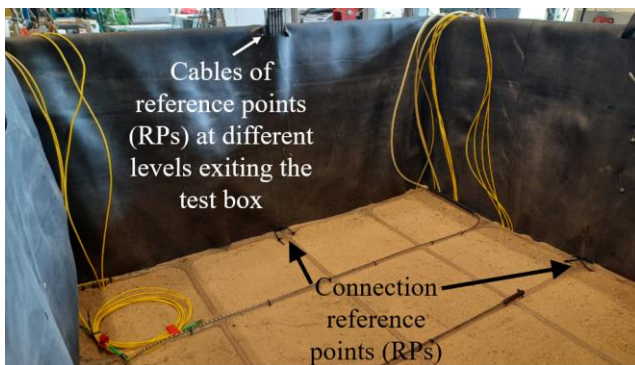


Figure 8. Overview with the reference points (RPs).

6 CONCLUSIONS

This paper dives into the DFOS measurements in four small-scale tests on steel-reinforced (SR) piled embankments. The DFOS results require considerable work to produce useful data for analyses.

This paper showed that local peaks occur in the data. These may be caused by local high pressures, resulting in local deviations in the measurements, but do not block the signal in the fibre. The paper provides some methods to deal with the spikes, including acceptance, interpolating and removal. It is important to further develop these methods to handle erroneous data more efficiently and ensure that the results obtained are reliable.

The paper also explains the steps necessary to get the *absolute* settlements along several lines at five elevations in the fill, during different test phases. For this purpose, *differential* strains were measured in four connected optic fibres, and the *absolute* settlements were measured at four reference points.

The paper shows how the innovative DFOS measurements gave an insightful and unique 3D

picture of the deformations and strains in a soil body, explains what work required to create these pictures from raw data, and discusses limitations in the accuracy of these measurements and their interpretation.

ACKNOWLEDGEMENTS

The authors are grateful for the funding received from the European Union's Horizon 2020 research and innovation program under Grant Agreement No. 101006512 for the transnational GEOLAB project PEBSTER, the TKI-PPS funding of the Dutch Ministry of Economic Affairs and the financial and practical support of Keller.

REFERENCES

- Bado, M.F., Casas, J.R., Gómez J. (2020). Post-processing algorithms for distributed optical fiber sensing in structural health monitoring applications. *Structural Health Monitoring I-20*.
- Bednarski, Ł., Sieńko, R., Grygierek, M., Howiacki, T. (2021). New Distributed Fibre Optic 3DSensor with Thermal Self-Compensation System: Design, Research and Field Proof Application Inside Geotechnical Structure. *Sensors* 21, 5089.
- Schneider, M., Hell, M., Wittekoek, B., Pandrea, P., van Eekelen, S.J.M., Topolnicki, M., Makowska, K., Sieńko, R., Zachert, H. (2024a). Large-scale test on the load bearing and deformation behaviour of basal steel-reinforced piled embankments. In: *Proc. ECSMGE 24*, Lisbon, Portugal.
- Schneider, M., Hell, M., Wittekoek, B., Pandrea, P., van Eekelen, S.J.M., Topolnicki, M., Makowska, K., Sieńko, R., Zachert, H. (2024b). High-density spatial measurements on a 3D large-scale model of a basal steel-reinforced piled embankment. In: *Proc. ECPMG*, Delft, Netherlands.
- Topolnicki, M., Sołtys, G., Brzozowski, T. (2019). Performance and modelling of road embankment supported on rigid inclusions and a transfer platform with steel geogrid, *Proc. of the ECSMGE 2019*, Reykjavik, Iceland.
- van Eekelen, S.J.M., Bezuijen, A., Lodder, H.J. & van Tol, A.F. (2012). Model experiments on piled embankments Part I. *Geotextiles and Geomembranes*, 32: 69-81.
- van Eekelen, S.J.M. and Han, J. (2020). Geosynthetic-reinforced pile-supported embankments: state of the art. *Geosynthetics International* 27 (2) 112-141.
- van Eekelen, S.J.M, Schneider, M., Hell, M., Wittekoek, B., Makowska, K., Zdanowicz, K., Pandrea, P., Sieńko, R., Schaubert, P., Topolnicki, M., Zachert, H. (2024). 3D small-scale tests on steel-reinforced piled embankments. In: *Proc. ECSMGE 24*, Lisbon, Portugal.
- Van Eekelen, S.J.M. (2024). Physical modelling of basal-reinforced pile-supported embankments. In: *Proc. ACPMG*, Abu Dhabi, UAE.

INTERNATIONAL SOCIETY FOR SOIL MECHANICS AND GEOTECHNICAL ENGINEERING



This paper was downloaded from the Online Library of the International Society for Soil Mechanics and Geotechnical Engineering (ISSMGE). The library is available here:

<https://www.issmge.org/publications/online-library>

This is an open-access database that archives thousands of papers published under the Auspices of the ISSMGE and maintained by the Innovation and Development Committee of ISSMGE.

The paper was published in the proceedings of the 5th European Conference on Physical Modelling in Geotechnics and was edited by Miguel Angel Cabrera. The conference was held from October 2nd to October 4th 2024 at Delft, the Netherlands.

To see the prologue of the proceedings visit the link below:

<https://issmge.org/files/ECPMG2024-Prologue.pdf>